Current Biology, Volume *29*

Supplemental Information

Distinct RhoGEFs Activate Apical and Junctional Contractility under Control of G Proteins during Epithelial Morphogenesis

Alain Garcia De Las Bayonas, Jean-Marc Philippe, Annemarie C. Lellouch, and Thomas Lecuit

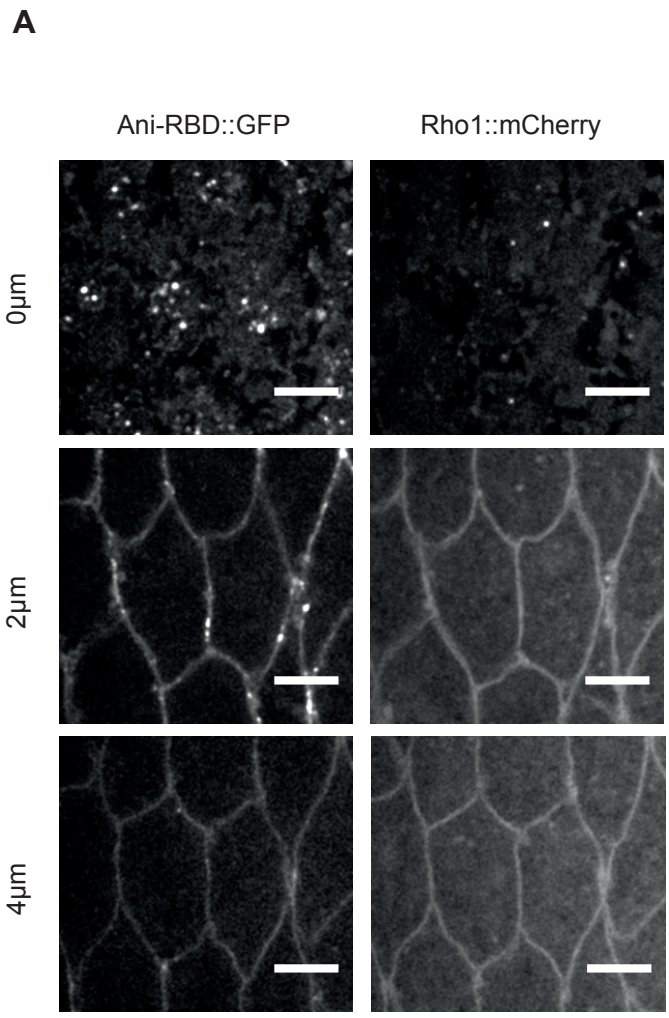
A
Ani-RBD::GFP
Rho1::mCherry
0µm
2µm
4µm
B
Intensity relative to junctional
1,05
1,00
0,95
0,90
0,85
0,80
0,75
0,70
2µm
3µm
4µm
Z plane (µm)
Rho1::mCherry
Ani-RBD::GFP
C
Amplitude of polarity
1,8
1,6
1,4
1,2
1,0
0,8
0,6
0,4
0,2
**
n=6 embryos
n=6 embryos
Rho1::mCherry
Ani-RBD::GFP

Figure S1. Rho1 protein is uniformly distributed in the ectoderm while its activity is polarized. Related to Figure 1.

(A) Apical (0µm), junctional (2µm) and lateral (4µm) confocal z-sections of ectodermal cells co-expressing Ani-RBD::GFP and Rho1::mCherry. Active Rho1 is enriched medial-apically and at junctions where it is planar-polarized. Rho1::mCherry signal is homogenous along the apico-basal axis. (B) Ani-RBD::GFP and Rho1::mCherry cortical levels normalized to the apical junctional intensities (2µm below the apical membrane) along the apico-basal axis. While Rho1::mCherry signal is uniform at cell cortex along the antero-posterior axis, active Rho1 is specifically enriched apically. (C) Quantification of Rho1::mCherry and Ani-RBD::GFP amplitude of polarity at junctions in the same embryos. A higher amplitude of polarity is measured for Ani-RBD::GFP at junctions compared to total Rho1. All the panels have the same orientation: dorsal at the top, anterior to the left. Scale bars = 5µm. Means ± SEM are shown. Statistical significance has been calculated using Mann-Whitney U test. ns, $p>0.05$; * $p<0.05$; ** $p<0.01$.

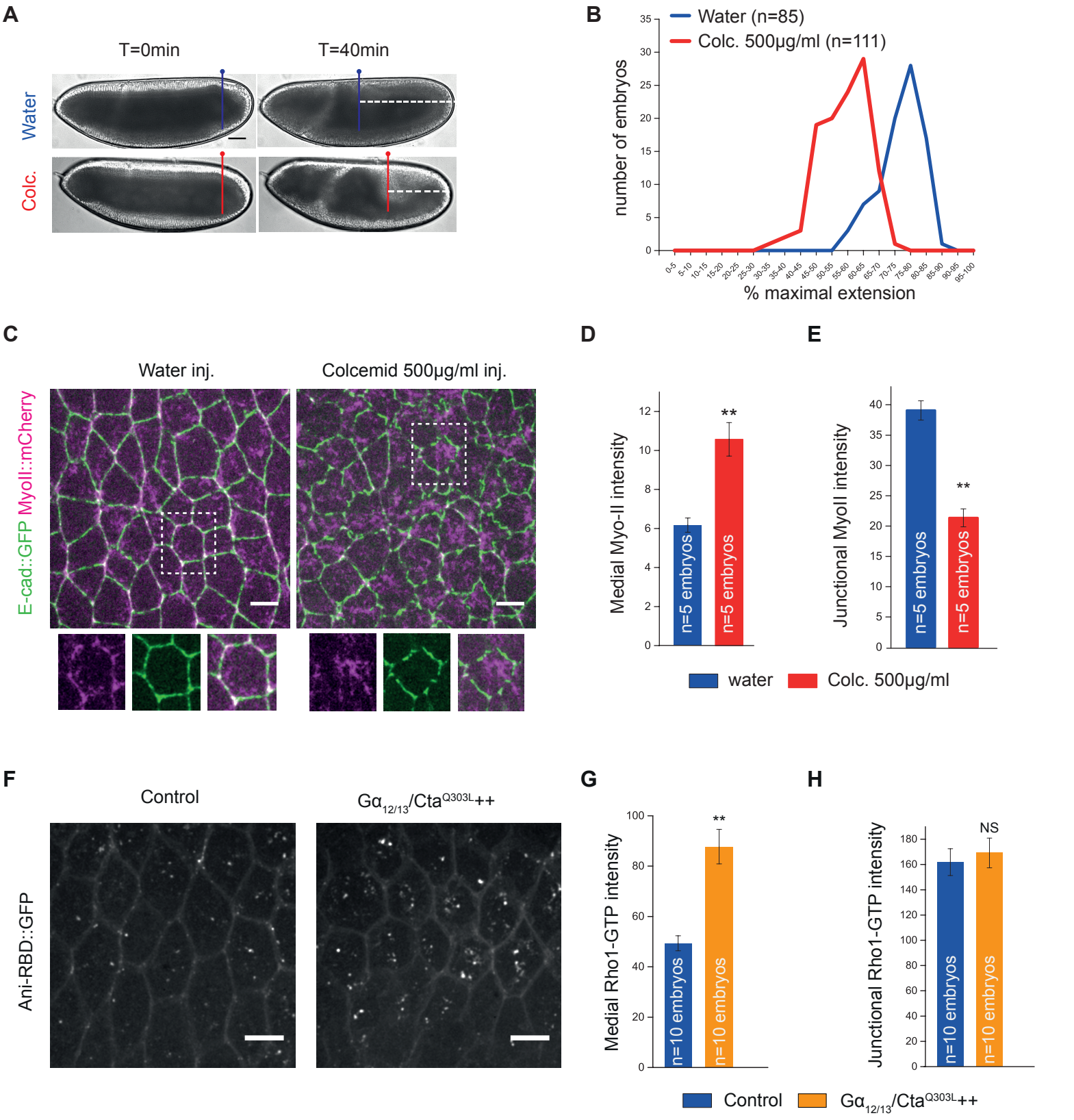
A
T=0min
T=40min
Water
Colc.
B
Water (n=85)
Colc. 500µg/ml (n=111)
number of embryos
% maximal extension
C
Water inj.
Colcemid 500µg/ml inj.
E-cad::GFP MyoII::mCherry
D
Medial Myo-II intensity
n=5 embryos
n=5 embryos
**
E
Junctional MyoII intensity
n=5 embryos
n=5 embryos
**
water
Colc. 500µg/ml
F
Control
Gα12/13/CtaQ303L++
Ani-RBD::GFP
G
Medial Rho1-GTP intensity
n=10 embryos
n=10 embryos
**
H
Junctional Rho1-GTP intensity
n=10 embryos
n=10 embryos
NS
Control
Gα12/13/CtaQ303L++

Figure S2. Microtubule depolymerization and $G\alpha_{12/13}/Cta^{Q303L}$ overexpression increases medial-apical Rho1 signaling. Related to Figure 2 and Videos S2 and S3.

(A) Lateral view of a water- and a colcemid-injected embryo at the onset (t=0min) of germ-band extension and 40min later. The dotted lines mark the distance between the pole cells and the posterior side of the embryos 40 minutes after the onset of germ-band extension. (B) Quantification of germ-band extension 40min after the onset of the process in water and colcemid-injected embryos. n=number of embryos. (C) Confocal acquisitions of water- and colcemid-injected embryos co-expressing Myo-II::mCherry and Endocad (E-cad)::GFP. A closeup of a representative cell is shown in the bottom part for both conditions. Colcemid-treated cells display higher medial-apical Myo-II levels and increased contractility. (D) Quantifications of mean medial-apical Myo-II intensities in both water- and colcemid-injected embryos. (E) Quantification of mean junctional Myo-II intensities in water and colcemid-injected embryos. (F) 4µm confocal z-projection of ventro-lateral ectodermal cells expressing Ani-RBD::GFP in control and $G\alpha_{12/}13$/CtaQ303L++ embryos. Active Rho1 is specifically increased in the medial-apical compartment of the cells upon $G\alpha_{12/}13$/CtaQ303L overexpression. (G,H) Mean medial-apical and junctional Rho1-GTP intensities in control and $G\alpha_{12/}13$/CtaQ303L++ embryos. All the panels have the same orientation: dorsal at the top, anterior to the left. Scale bars = 50µm (A) and =5µm (C and E). Means ± SEM are shown. Statistical significance has been calculated using Mann-Whitney U test. ns, $p>0.05$; * $p<0.05$; ** $p<0.01$.

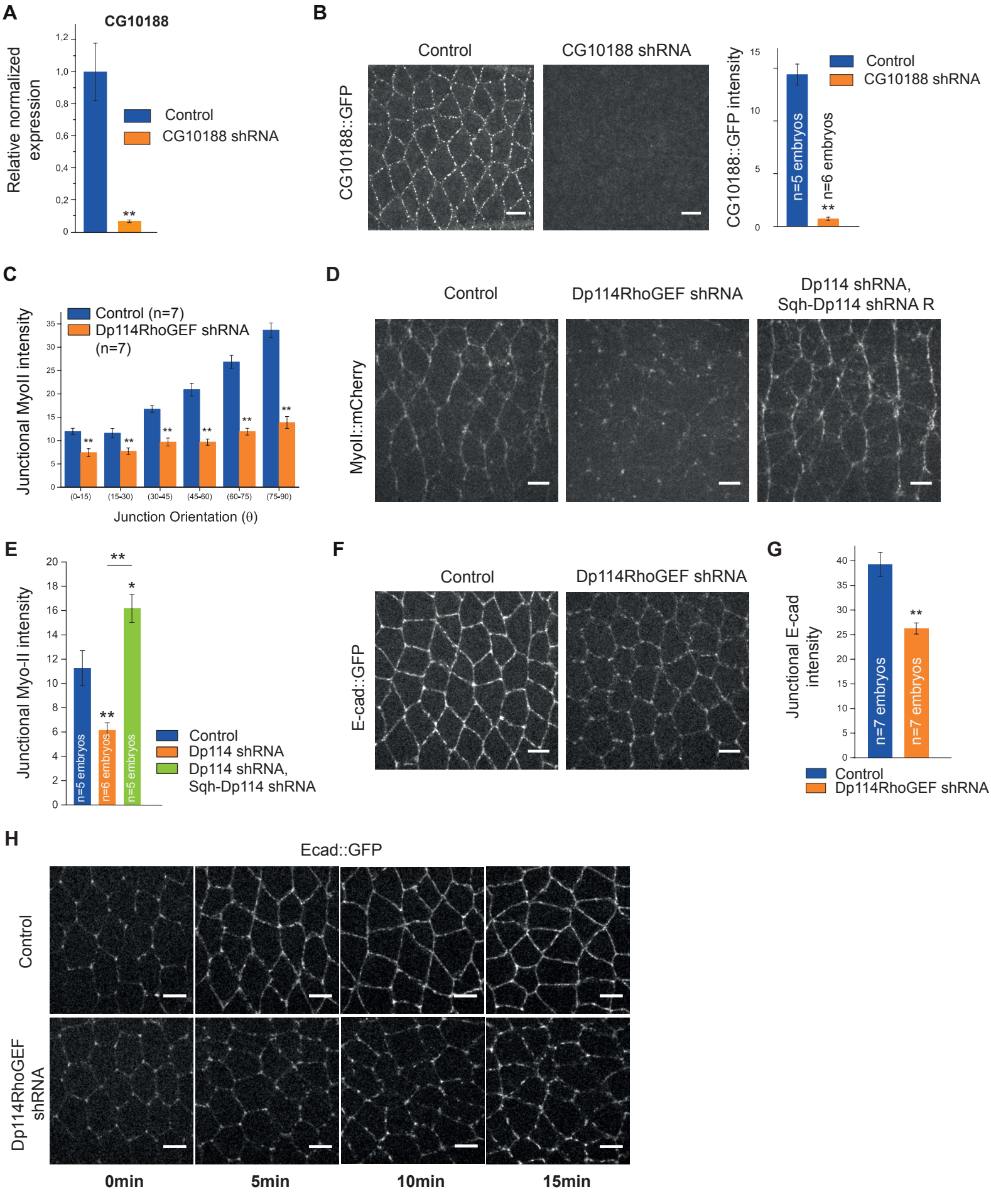
A
CG10188
Relative normalized expression
1,2
1,0
0,8
0,6
0,4
0,2
0
**
Control
CG10188 shRNA
B
Control
CG10188 shRNA
CG10188::GFP
CG10188::GFP intensity
15
10
5
0
n=5 embryos
n=6 embryos
**
Control
CG10188 shRNA
C
Junctional MyoII intensity
Control (n=7)
Dp114RhoGEF shRNA (n=7)
35
30
25
20
15
10
5
0
**
(0-15)
(15-30)
(30-45)
(45-60)
(60-75)
(75-90)
Junction Orientation (θ)
D
Control
Dp114RhoGEF shRNA
Dp114 shRNA, Sqh-Dp114 shRNA R
MyoII::mCherry
E
Junctional Myo-II intensity
20
18
16
14
12
10
8
6
4
2
0
**
*
n=5 embryos
n=6 embryos
n=5 embryos
Control
Dp114 shRNA
Dp114 shRNA, Sqh-Dp114 shRNA
F
Control
Dp114RhoGEF shRNA
E-cad::GFP
G
Junctional E-cad intensity
40
35
30
25
20
15
10
5
0
**
n=7 embryos
n=7 embryos
Control
Dp114RhoGEF shRNA
H
Ecad::GFP
Control
Dp114RhoGEF shRNA
0min
5min
10min
15min

Figure S3. Myo-II and E-cadherin junctional levels are affected in Dp114RhoGEF knock-down embryos. Related to Figures 3 and 4, and Video S5.

(A) RT-qPCR showing the knock-down of CG10188 transcripts in maternally expressed CG10188 shRNA compared to control embryos. A 14-fold depletion of the *CG10188* transcripts is observed. (B) Left panels: Confocal z-projection of Sqh-eGFP::CG10188 embryos (control) and Sqh-eGFP::CG10188 embryos co-expressing CG10188 shRNA. The protein is almost absent in the latter case. A quantification of eGFP::CG10188 protein signal in both conditions is depicted in the right panel. (C) Mean junctional intensity of Myo-II according to the angle of the junctions in control and Dp114RhoGEF shRNA expressing embryos. (junction angle; 0°, parallel to the antero-posterior axis; 90°, perpendicular to the antero-posterior axis). n= number of embryos. A global decrease in Myo-II is observed at both transverse and vertical interfaces. (D) Confocal projections of embryos expressing Sqh::mCherry in control background (left panel), Dp114RhoGEF shRNA background (middle panel) and in genetic background where Dp114RhoGEF shRNA is co-expressed with a modified form of the Dp114RhoGEF mRNA immune to targeting by the Dp114RhoGEF shRNA (SqhPa-Dp114RhoGEF -shRNA^{R}) (right panel). Note that Myo-II cables are rescued in the last condition (right panel) compared with middle panel. (E) Quantification of mean junctional Myo-II intensities in control, Dp114RhoGEF shRNA and Dp114RhoGEF shRNA, Sqh-Dp114RhoGEF shRNA^{R}. (F) Confocal projections of ectoderm tissues expressing E-cad::GFP in control and Dp114RhoGEF shRNA embryos. E-cadherin junctional levels are decreased upon Dp114RhoGEF depletion. (G) Mean E-cadherin junctional intensities. (H) E-cad::GFP in time lapse videos of control (top panels) and Dp114RhoGEF shRNA embryos (bottom panels) (t=0 is the end of the mesoderm pulling). Anterior is left and ventral is down. E-cadherin is enriched at cell vertices in the early germ-band and rapidly accumulates along junctions where it forms an adhesive belt in control embryos. In Dp114RhoGEF shRNA embryos, E-cadherin junctional maturation is disrupted and shows a low and discontinuous signal. Scale bars = 5µm. Means ± SEM are shown. Statistical significance has been calculated using Mann-Whitney U test. ns, $p>0.05$; * $p<0.05$; ** $p<0.01$.

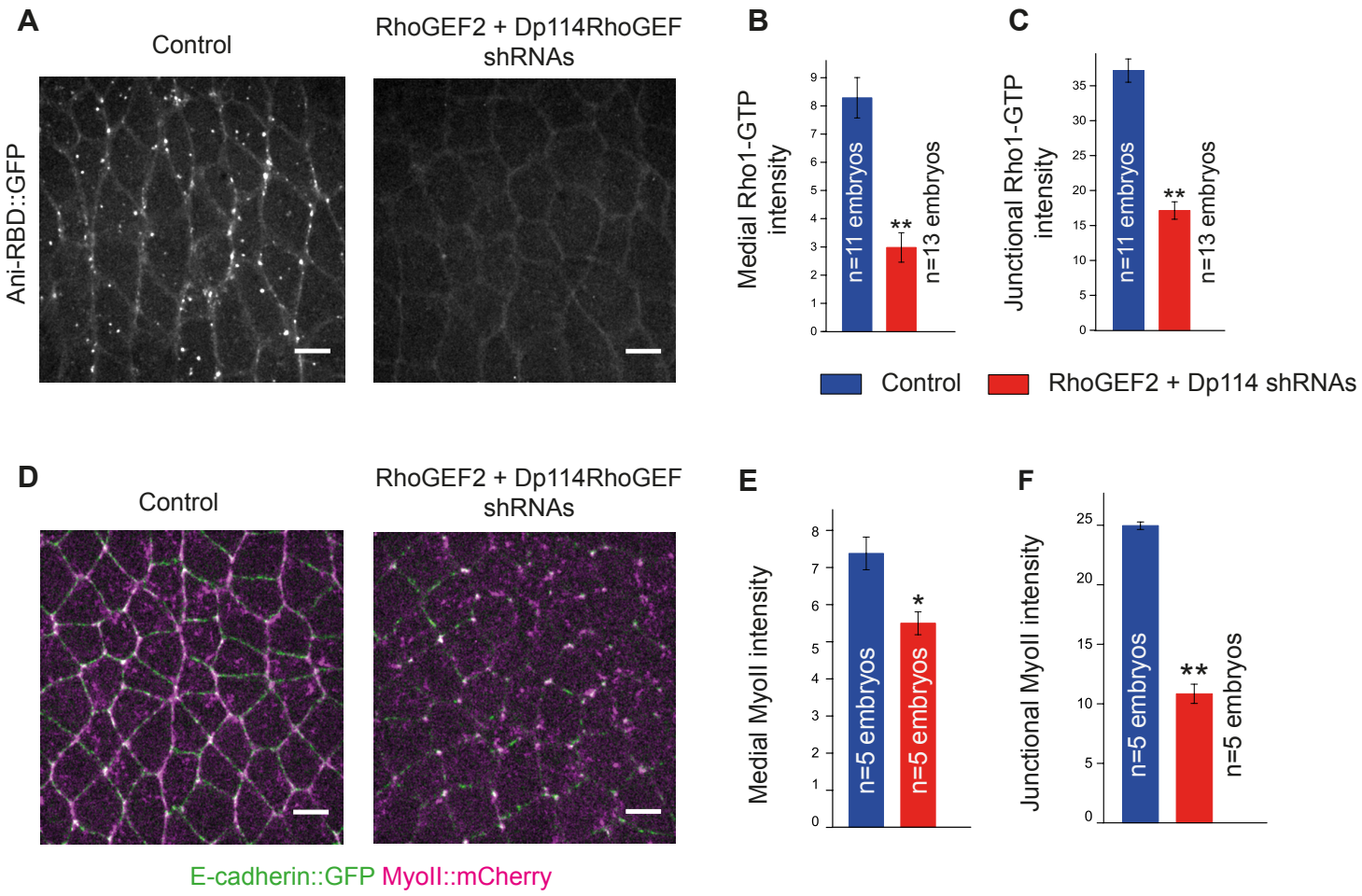
A
Control
RhoGEF2 + Dp114RhoGEF shRNAs
Ani-RBD::GFP
B
Medial Rho1-GTP intensity
n=11 embryos
n=13 embryos
**
C
Junctional Rho1-GTP intensity
n=11 embryos
n=13 embryos
**
Control
RhoGEF2 + Dp114 shRNAs
D
Control
RhoGEF2 + Dp114RhoGEF shRNAs
E-cadherin::GFP MyoII::mCherry
E
Medial MyoII intensity
n=5 embryos
n=5 embryos
*
F
Junctional MyoII intensity
n=5 embryos
n=5 embryos
**

Figure S4. RhoGEF2 and Dp114RhoGEF double knock-down decreases both medial-apical and junctional Rho1 signaling. Related to Figure 1 and 4.

(A) Confocal z-projections of control and RhoGEF2 + Dp114RhoGEF double knock-down embryos (RhoGEF2+ Dp114RhoGEF shRNAs) expressing Ani-RBD::GFP. A decrease in both medial-apical and junctional Rho1 activity is observed in the second condition. (B, C) Mean medial-apical and junctional Rho1-GTP intensities in control and RhoGEF2+ Dp114RhoGEF shRNAs embryos. (D) 5µm confocal z-projections of ventro-lateral ectodermal cells expressing E-cad::GFP and MyoII::mCherry in control and RhoGEF2+ Dp114RhoGEF shRNAs embryos. Similar to the previous observations, medial-apical and junctional Myo-II pools are decreased in mutant embryos. (E, F) Mean medial-apical and junctional Myo-II intensities. Scale bars = 5µm. Means ± SEM are shown. Statistical significance has been calculated using Mann-Whitney U test. ns, $p>0.05$; * $p<0.05$; ** $p<0.01$.

A

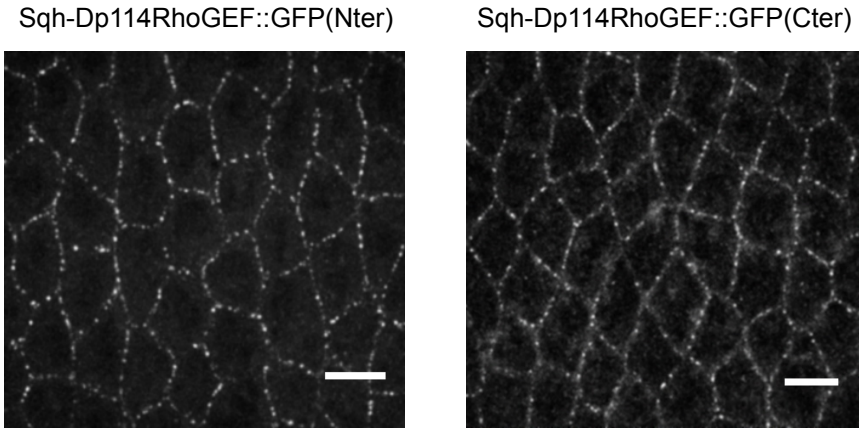
Sqh-Dp114RhoGEF::GFP(Nter)
Sqh-Dp114RhoGEF::GFP(Cter)

B

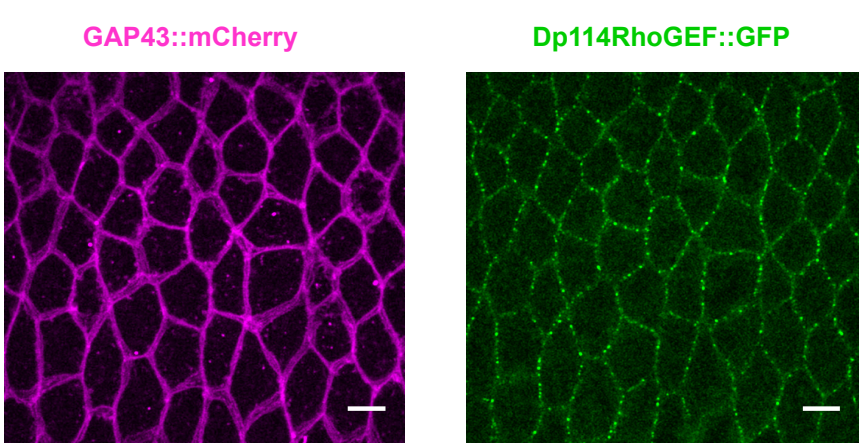
GAP43::mCherry
Dp114RhoGEF::GFP

C

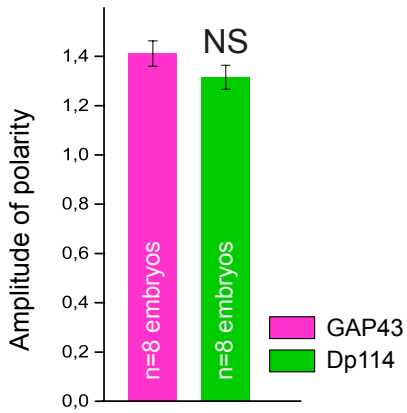
Amplitude of polarity
1,4
1,2
1,0
0,8
0,6
0,4
0,2
0,0
NS
n=8 embryos
n=8 embryos
GAP43
Dp114

Figure S5. GFP-tagged Dp114RhoGEF localizes at cell junctions with no apparent planar-polarity. Related to Figure 7.

(A) Confocal z-projections of ectodermal cells expressing Dp114RhoGEF tagged with GFP at its N-terminal (left panel) or C-terminal end (right panel). Although both fusion proteins localize at adherens junctions, a stronger cytoplasmic signal is often observed in embryos expressing the Dp114RhoGEF construct tagged in C-ter. Dp114RhoGEF tagged in N-ter has been used hereafter. (B) 4µm confocal z-projection of ectodermal cells co-expressing the membrane marker GAP43::mCherry and Dp114RhoGEF::GFP in the same embryo. (C) Quantification of GAP43 and Dp114RhoGEF amplitude of polarity in the same embryos. Dp114RhoGEF::GFP polarity at junctions is similar to the polarity of the membrane marker. Scale bars = 5µm. Means ± SEM are shown. Statistical significance has been calculated using Mann-Whitney U test. ns, $p>0.05$; * $p<0.05$; ** $p<0.01$.

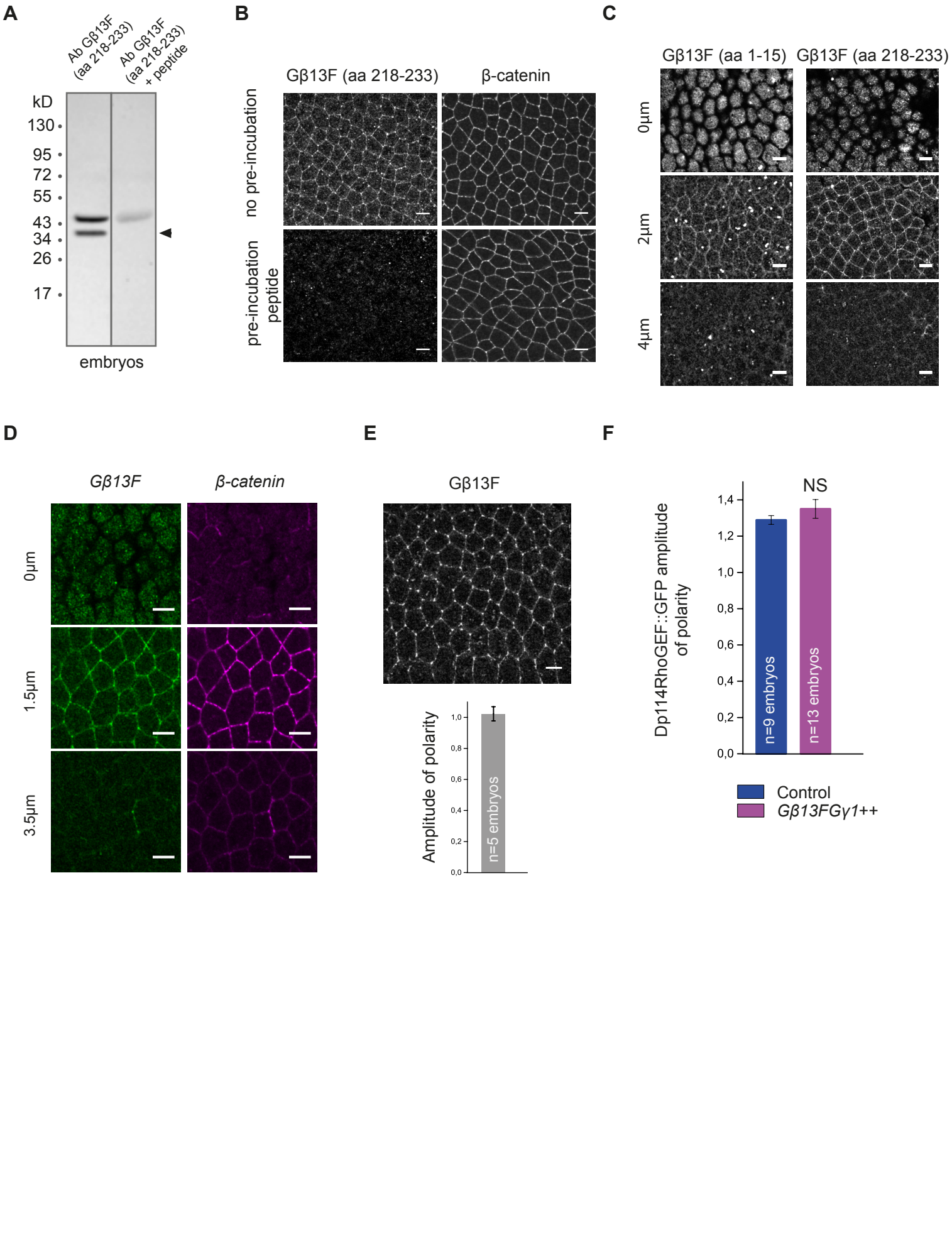
A
Ab Gβ13F (aa 218-233)
Ab Gβ13F (aa 218-233) + peptide
kD
130
95
72
55
43
34
26
17
embryos
B
Gβ13F (aa 218-233)
β-catenin
no pre-incubation
pre-incubation peptide
C
Gβ13F (aa 1-15)
Gβ13F (aa 218-233)
0µm
2µm
4µm
D
Gβ13F
β-catenin
0µm
1.5µm
3.5µm
E
Gβ13F
Amplitude of polarity
n=5 embryos
F
Dp114RhoGEF::GFP amplitude of polarity
NS
n=9 embryos
n=13 embryos
Control
Gβ13FGγ1++

Figure S6. Gβ13F localizes apically and at adherens junctions with no planar-polarity in the ectoderm. Related to Figure 7.

(A) Gβ13F (218-233) antibody specificity of binding was analyzed further in immunoblotting on *yw* embryos lysates. Two bands were detected: one at the expected Gβ13F molecular weight (37kDa, black arrow) and another band around 45 kDa. Importantly, the 37kDa band was abolished when the membrane was pre-treated with the blocking Gβ13F (218-233) peptide. The higher molecular weight band was strongly diminished but not completely removed. (B) Ventro-lateral ectoderms stained with Gβ13F (218-233) and β-catenin antibodies. Pre-incubation of the Gβ13F (218-233) antibody with the Gβ13F (218-233) peptide completely abolished Gβ13F signal (left bottom panel). (C) Apical (0µm), junctional (2µm) and lateral (4µm) confocal z-sections of ectodermal cells in fixed embryos stained with two different purified antibodies against Gβ13F (see material and methods). Both antibodies showed a similar staining, with Gβ13F being enriched apically and at adherens junctions. Because antibody against the Gβ13F (218-233) peptide gave a cleaner staining with less intracellular aggregates, we performed the next experiments using this purified antibody exclusively. (D) Apical (0µm), junctional (1.5µm) and lateral (3.5µm) confocal z-sections of ectodermal cells in fixed embryos stained with Gβ13F and β-catenin antibodies. Gβ13F co-localizes with β-catenin at junctions. (E) Quantification of the amplitude of polarity of Gβ13F measured on fixed embryos. Gβ13F is not planar-polarized at cell junctions. (F) Quantifications of Dp114RhoGEF::GFP amplitude of polarity in control and Gβ13FGγ1 overexpressing embryos (Gβ13FGγ1++). While Gβ13FGγ1 overexpression increases Dp114RhoGEF::GFP levels at cell junctions (see main Figures 7 F and 7G), its amplitude of polarity is not affected. Scale bars = 5µm.

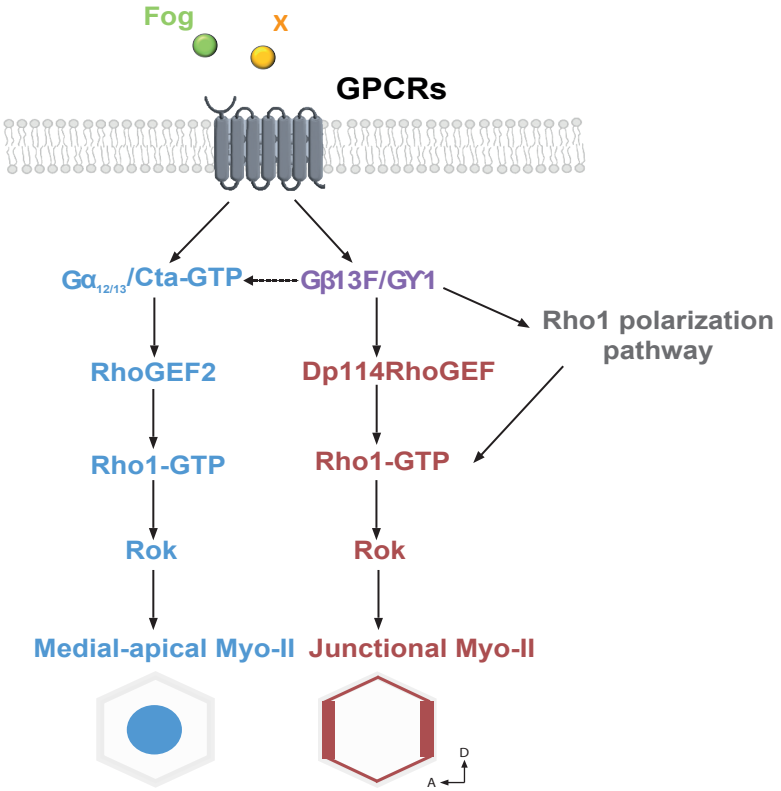
Fog
X
GPCRs
Gα12/13/Cta-GTP
Gβ13F/Gγ1
Rho1 polarization pathway
RhoGEF2
Dp114RhoGEF
Rho1-GTP
Rho1-GTP
Rok
Rok
Medial-apical Myo-II
Junctional Myo-II
D
A

Figure S7. Distinct RhoGEFs compartmentalize Rho1 signaling apically and at junctions under control of G proteins in the *Drosophila* embryonic ectoderm. Related to Figures 1 and 2 and Figures 4-7.

An overview of the medial (in blue) and junctional (in red) signaling pathways controlling Rho1 activity in the ectoderm. Following stimulation by ligand (Fog and others), GPCRs release active $G\alpha_{12/13}$/Cta ($G\alpha_{12/13}$/Cta -GTP) and active Gβ13FGγ1 dimers that promote RhoGEF2 and Dp114RhoGEF signaling respectively. Note that Gβ13FGγ1 favors indirectly medial-apical signaling by localizing $G\alpha_{12/13}$/Cta at the membrane allowing it to signal downstream of GPCR activation (dotted arrow). How Gβ13FGγ1 polarize junctional Rho1 activation is unclear and could involve Toll receptors.